2018

Experimental Analysis and Design Improvements on Combined Viper Expansion Work Recovery Turbine and Flow Phase Separation Device Applied in R410A Heat Pump

Riley Barta
Purdue University, bartar@purdue.edu

Florian Simon
Purdue University, United States of America, florian_simon_91@icloud.com

Eckhard A. Groll
Purdue University - Main Campus, groll@purdue.edu

Experimental Analysis and Design Improvements on Combined Viper Expansion Work Recovery Turbine and Flow Phase Separation Device Applied in R410A Heat Pump

Riley B. BARTA[1*], Florian SIMON[1], and Eckhard A. GROLL[1]

[1]Ray W. Herrick Laboratories, School of Mechanical Engineering, Purdue University
West Lafayette, Indiana, 47906, USA
bartar@purdue.edu; florian_simon_91@icloud.com; groll@purdue.edu

ABSTRACT

In light of recent trends towards energy efficiency and environmental consciousness, the heating, ventilation, air conditioning and refrigeration (HVAC&R) industry has been pushing for technological developments to meet both of these needs. As such, several solutions for harnessing the energy released from refrigerants during the free expansion process of a conventional vapor-compression cycle have been developed to increase overall cycle efficiency. The goal of this research is to investigate the potential impact of installing an energy recovery expander, named Viper Expander, into an R410A heat pump cycle and to increase the efficiency of the expander. To improve the expander design, flow visualization of the two-phase refrigerant leaving the nozzle has been performed. Additionally, a housing redesign that would allow the expander to act as both an expansion work recovery device as well as a flash tank economizer has been proposed and tested as a system solution. Implementing phase separation is intended to have the combined effect of reducing turbine performance losses while also serving as an open economizer to increase overall cycle performance. An experimental investigation of these effects is presented herein, with preliminary experimental results of an expander isentropic efficiency of 18%.

1. INTRODUCTION

With increasing demand for high-efficiency vapor-compression cycles, all components of the cycle are being considered for potential performance increases. The process of the cycle that expands the refrigerant from high-pressure at the condenser outlet to low-pressure at the evaporator inlet is one area of recent interest for performance gains. The majority of vapor-compression cycles in production today, especially those utilizing hydrofluorocarbon (HFC) refrigerants such as R410A, use either a thermostatic expansion valve (TXV) or an electronic expansion valve (EXV) for the expansion process, neither of which harvests any of the energy lost during the expansion. Additionally, economization in vapor-compression cycles has been increasingly investigated due to the same energy-conscious trends.

The expander device was developed in order to replace the TXV or EXV found in traditional vapor-compression cycles, and it consists of three main components. In particular, the first is the nozzle that converts the potential energy in the high-pressure refrigerant into a high-velocity stream, which then impinges on the second component, the turbine. This turbine is directly connected to the third component, the generator, by a shaft. As the turbine spins, it also spins the generator, thus producing alternating current (AC) power. This AC power is then rectified to direct current (DC) before travelling through a variable resistance bank to allow simulation of loading of the generator. Potential use for the power recovered from the expander would likely be one of the fans in the refrigeration system, which would have a DC power input.

The development of expansion work recovery devices has been pursued using several techniques and working fluids. Baek *et al.* (2002) designed and tested a prototype piston-cylinder expansion device in a transcritical CO_2 cycle and increased the system performance by up to 10%. Wang *et. al* (2012) described a vane type expander for an R410A refrigeration system and found a potential coefficient of performance (COP) improvement of 14.2% through simulation of the system. Turbomachinery expanders have also begun to be investigated as a potential method for expansion work recovery. He *et al.* (2009) reached an isentropic efficiency of 32.8% and a COP improvement of 5.4% using a turbo expander in an R410A domestic refrigeration system.

One of the primary forms of economization, referred to as open economization, is often achieved through the use of a component called a flash tank. The other form of economization is called closed economization, an example of which

uses an internal heat exchanger. In a flash tank the two-phase refrigerant at the inlet is separated using gravity, and the saturated liquid is sent from the bottom of the flash tank to the evaporator while the saturated vapor is sent out the top of the flash tank directly to the compressor. Wang *et al.* (2009) compared open and closed economization applied to compressor vapor injection in an R410A heat pump and found that open and closed economization had similar performance benefits overall in cooling mode, with a maximum COP increase of 2-4%. However, in heating mode a maximum COP increase of 23% was found using open economization. Zhang and Tian (2014) presented an expansion device design serving as an economizer for vapor injection and expansion work recovery device at the same time. By separating liquid and vapor it was found via simulation that the friction losses of the impeller became significantly smaller and resulted in a 20% improvement in isentropic efficiency. This device was based on a patent by Sakata *et al.* (1984). Work by Tondell (2006) resulted in a relationship displayed by Equation 1, which describes the friction loss of a turbo expander as a function of density, rotational velocity, blade height, disk friction and two empirical coefficients, and this equation supports to goal of reducing density of the fluid in the turbine.

$$N_{rot} = \rho\omega^3 \mathrm{R}^4(\mathrm{k}_1\mathrm{R} + \mathrm{k}_2\mathrm{H}) \quad (1)$$

This research is motivated by the unique ability for the proposed expander device to provide a combination of two potential solutions, expansion work recovery and economization, to the given challenge of increasing the efficiency of heat pump cycles. In fact, the expander can provide experimental validation for the concept of a combined expansion work recovery device and an open economizer. Furthermore, this design has the added benefit of removing liquid from the turbine, which serves as a solution to reducing friction on the impeller due to phase separation. The inclusion of separate outlets for liquid and vapor in the expander housing, which are sent to the evaporator inlet and outlet, respectively, enables an increase in change in enthalpy across the evaporator and a reduction in compressor suction temperature, both of which have the potential to increase cycle efficiency. An overview of the modeling used in the expander housing redesign as well as preliminary experimental results is provided. Upper and lower limits of cycle operating conditions were considered to ensure the liquid level in the expander housing remained at safe values. The experimental setup is described, and experimental results concerning both expander effectiveness as an expansion work recovery device and an open economizer are presented. Future work regarding improvements on the housing, nozzle, turbine, and vapor bypass valve is identified.

2. THEORETICAL APPROACH

A primary focus of the expander housing redesign was to ensure that the housing height allowed for safe liquid levels over the range of operating conditions analyzed. The height of the housing was the primary parameter being varied, as the diameter of the housing was fixed as a function of turbine outer diameter and the distance between the turbine outer diameter and the housing inner diameter. Therefore, the housing volume is varied solely as a function of height in this analysis. The two extreme conditions considered were the liquid level becoming so low that two phase was able to exit through the liquid outlet, thus compromising evaporator performance, and the liquid level becoming too high and hitting the bottom of the turbine, thus decreasing the rotational velocity of the turbine. The housing height was chosen with an input of the minimum liquid height over the range of operating conditions, and this height was simulated with conditions resulting in maximum liquid level to ensure that the liquid never reached the bottom of the turbine. All of these calculations were performed based on the assumption of ideal phase separation. The housing calculations were performed in a steady-state thermodynamic cycle model using Engineering Equation Solver (EES), Klein (2018).

The modeled cycle consists of a single-stage compressor, condenser, expander, flash tank, vapor bypass line, and an evaporator. A schematic of the cycle is shown in Figure 1, and a P-h diagram of the cycle is shown in Figure 2. The cycle is operated in cooling mode due to the larger pressure differential across the expansion process, which results in a higher potential for expansion work recovery. The evaporation temperature is a function of the indoor temperature, the compressor suction superheat, and the approach temperature between the air and the refrigerant. Similarly, the condensing temperature is a function of the ambient temperature, the condenser outlet subcool, and the approach temperature between the air and the refrigerant. Several of these parameters were varied, however a fixed heat exchanger approach temperature of 5 ℃ was assumed for the cycle. Compressor performance and operating conditions were governed by an isentropic efficiency, as shown in Equation 2. A compressor isentropic efficiency of 70% was assumed for the range of the parametric study.

$$\eta_{comp} = \frac{h_{out,s} - h_{in}}{h_{out} - h_{in}} \quad (2)$$

where

$$h_{out,s} = f(p_{out}, s_{in}) \quad (3)$$

Similarly, the expander performance was simulated with an isentropic efficiency calculated with Equation 4.

$$\eta_{exp} = \frac{h_{in} - h_{out}}{h_{in} - h_{out,s}} \quad (4)$$

Pressure drop and heat loss throughout the refrigerant lines and components were neglected. The expander outlet state was assumed to be equal to the flash tank inlet state and thus, the quality of the flash tank was known due to the assumption that the flash tank and evaporation pressures were equal. By using this quality, the specific volume of the saturated liquid and vapor in the flash tank, and the expander dimensions (see Figure 3), a parametric study was conducted to find a value for H_1 that would prevent too much or too little liquid in the expander housing. This was ultimately possible due to the assumption that the flash tank in this model represented the flash tank portion of the modified expander housing. The turbine diameter D_t, the distance between generator and the top of the housing, H_3, the height of the generator turbine unit, H_2, and the inner housing diameter D_h, are defined by generator design and are fixed constraints. Therefore, H_1 was left as a variable and was calculated as a function of liquid and vapor height in the housing. To identify a safe H_1 that would prevent the liquid level from both falling below 10 mm and rising high enough to hit the turbine, the cycle model was run with a parametric study conducted over a range of operating conditions and key variables summarized in Table 1. The results will be discussed in Section 4.2.

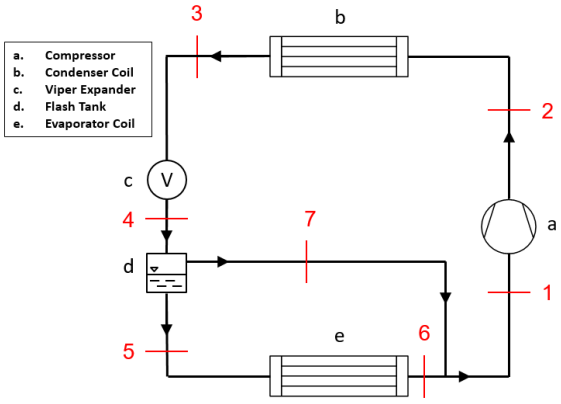

Figure 1: Schematic of expander heat pump cycle

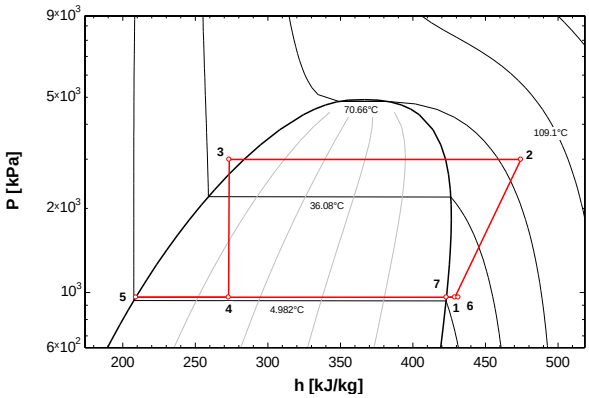

Figure 2: Expander Heat pump cycle in a P-h diagram

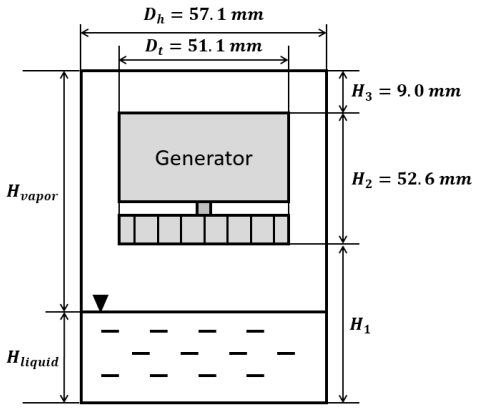

Figure 3: Dimensions of the new expander housing

Table 1: Min and max values for parameters varied in expander housing parametric study

Parameter	Units	Minimum Value	Maximum Value
$T_{ambient}$	[°C]	19	35
T_{indoor}	[°C]	18	23
$\Delta T_{subcool}$	[°C]	2	8
$\Delta T_{superheat}$	[°C]	3	10
η_{exp}	[-]	0.07	0.7

3. EXPERIMENTAL SETUP

3.1 Flow Visualization Setup

The first step in assessing where performance losses in the expander were occurring was to understand the shape of the flow at the outlet of the nozzle so that the turbine could be better designed and placed to harvest kinetic energy more efficiently from the flow. To make this flow visualization possible, a high-pressure sight glass was installed in parallel with the TXV and expander in the expansion portion of the 5-ton R410A heat pump that was used for this testing. A customized interface between the nozzle and sight glass was machined so that the nozzle tip could be seen through the glass, allowing visualization of the entire flow starting at the exit of the nozzle. A schematic and photo of this setup is shown in Figures 4 and 5, respectively.

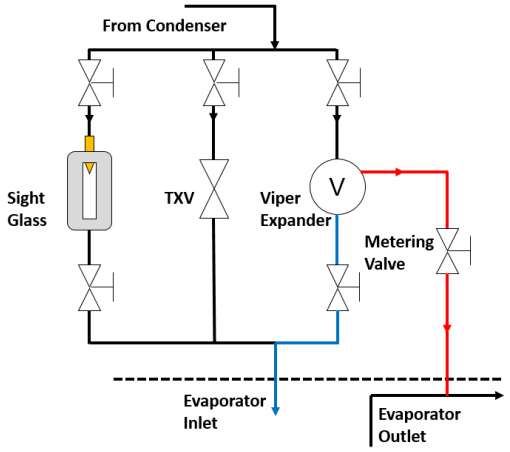

Figure 4: Schematic of expansion circuit

Figure 5: Photo of nozzle visualization sight glass

3.2 Expander Heat Pump Experimental Setup

The expander testing was performed using a 5-ton unitary split-system heat pump in two psychrometric chambers. This allowed independent control of both the temperature and relative humidity for the environment around both the indoor and outdoor unit of the heat pump. The two cooling mode operating conditions used in preliminary testing were from ANSI/AHRI Standard 210/240 (2008) and are outlined in Table 2. A schematic of the expander experimental setup as well as the instrumentation utilized is shown in Figure 6. An EES model of a 4-component vapor-compression cycle was used for data analysis, and measurements from all state points shown in Figure 6 were input into the code to analyze the cycle. Because the power output from the expander was a measured value, Equation 5 was used to calculate overall isentropic efficiency of the expander.

$$\eta_{exp,o} = \frac{\dot{W}_{exp}}{\dot{m}(h_{in} - h_{out,s})} \tag{5}$$

Table 2: ANSI/AHRI Standard 210-240

Condition	Dry Bulb Temperature [°C]		Relative Humidity [%]	
	Indoor	Outdoor	Indoor	Outdoor
A	26.7	35	51.1	39.8
B	26.7	27.8	51.1	39.8

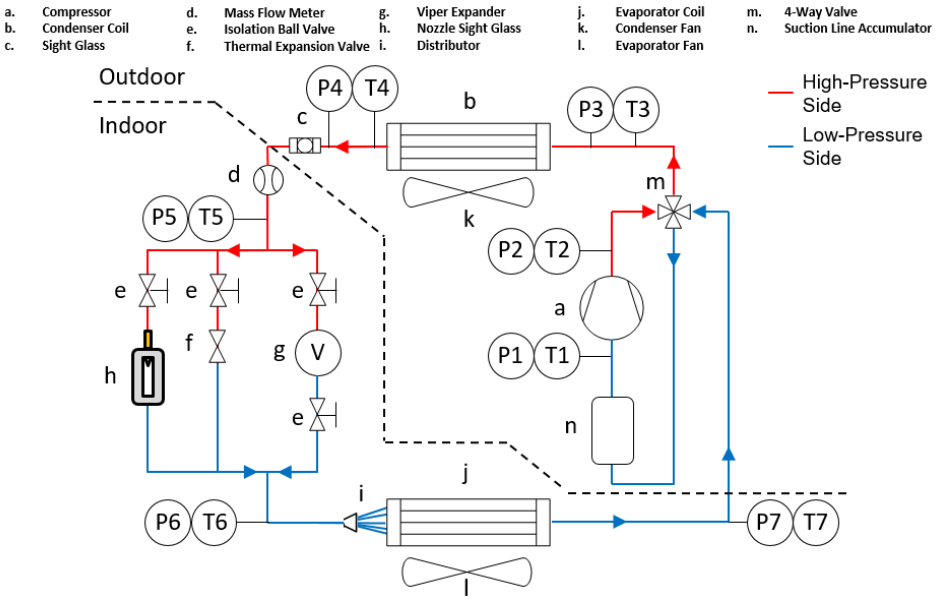

Figure 6: 5-Ton heat pump and psychrometric chamber schematic

To calculate all thermo-physical properties of the cycle at key state points, pressure transducers and thermocouples were utilized. In addition, watt transducers were installed to measure fan and compressor power consumption. A Coriolis-effect mass flow meter was placed in the liquid line to measure refrigerant mass flow rate. To measure expander performance, a watt multiplier and a frequency transducer were used to measure power output and frequency of the output, respectively.

4. RESULTS AND DISCUSSION

4.1 Flow Visualization Results

Using the previously-described flow visualization setup, the flow exiting a converging-diverging (C-D) nozzle was able to be visualized during the expansion process of the R410A heat pump. The slow motion video used allowed the capture of images immediately following the flow travelling through a C-D nozzle with a throat diameter of 2.79 mm. The photos are shown in Figure 7a through 7c, being the first and the final snapshots, respectively, over the span of 2 seconds. A time span of 2 seconds was chosen because this was the period of time it took for the shape of the flow to be difficult to see due to the splashing of two-phase refrigerant and oil on the sides of the sight glass.

Due to precise measurements necessary for accurate calculation of geometry, the primary takeaways from these photos were observations regarding the shape, distance before the flow lost a distinct shape, and phase of the flow. It can be seen by the first two photos of Figure 7 that the inlet shape is a cone. The nozzle outlet flow becomes too dispersed to reliably calculate its dimensions at a distance of 11 mm from the nozzle tip, at which point the diameter of the flow is 3.5 mm. These two measurements, in combination with the nozzle geometry drawings, allowed for a cone shape of the flow to be placed over a drawing of the turbine and housing before modification, as shown in Figure 8a.

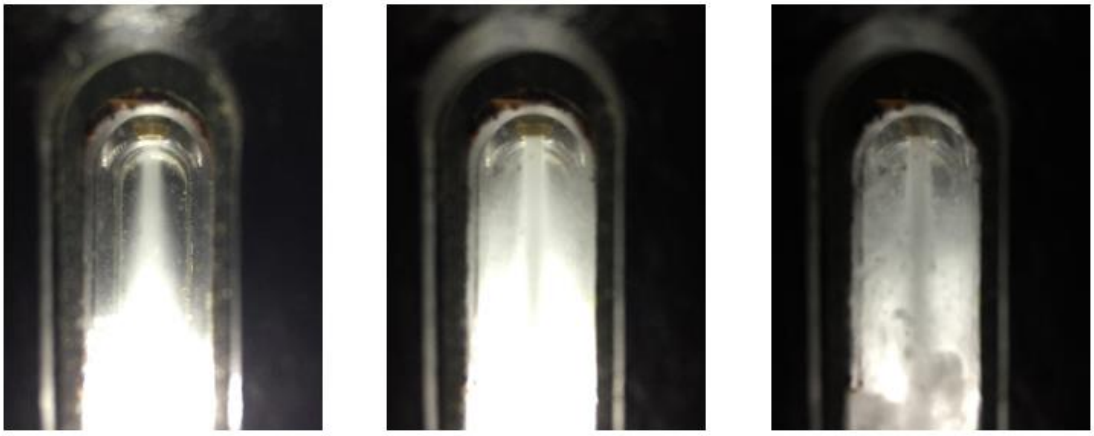

a) Initial photo b) Second time step photo c) Final photo

Figure 7: Development of flow at nozzle outlet over 2 seconds

After investigating the potential negative effects of where the majority of the flow cone was hitting the turbine blades, the nozzle was moved to the right 0.95 mm with respect to the center, as shown in Figure 8b. Figure 7c shows a final photo taken of the flow before the entire glass became enveloped in two-phase flow splashing up the sides. While it was discussed that a portion of the splashing fluid is oil, the violent mixing appeared to create significant turbulence. This inspired the concern that this two-phase separation turbulence could adversely affect the performance of the turbine, and the idea of separating the saturated liquid and saturated vapor in the same housing as the turbine was harvesting energy became a focus of the housing redesign.

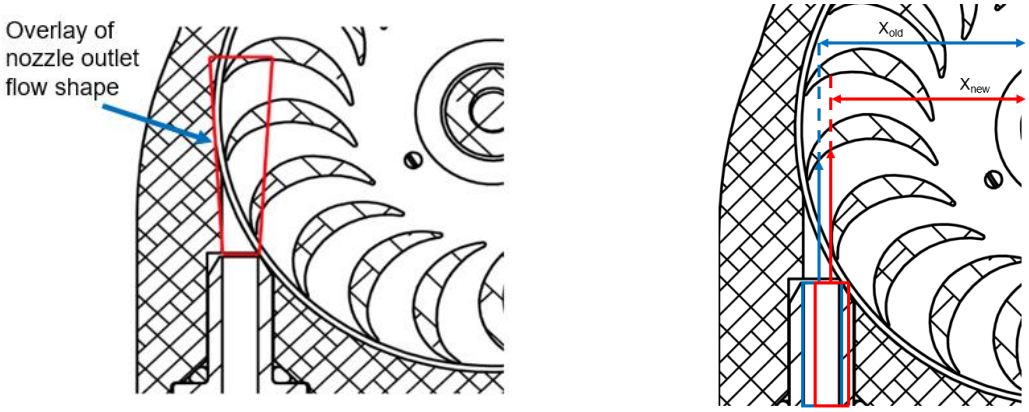

a) Nozzle flow shape overlay b) Nozzle repositioning in housing

Figure 8: Flow geometry overlay on turbine drawing

4.2 Housing Redesign

An overview of the initial and modified expander housings is provided in Figure 9. In particular, Figure 9a shows the initial expander housing with a radial inlet and single axial outlet, a smaller gap between the turbine outer diameter and housing inner diameter, and no extra space for phase separation. Figure 9b shows the modified housing with the radial inlet and two outlets, a larger gap between the turbine outer diameter and housing inner diameter, and space in the bottom for the liquid to pool. To be noted is that these figures are not to scale, and the repositioning of the nozzle is not visible. In the modified expander housing, the two-phase mixture is expanded through a nozzle before it enters the turbine radially and leaves axially. The liquid phase refrigerant is gathered in the bottom of the housing, where it

exits the housing and eventually mixes with the evaporator outlet refrigerant flow. The vapor travels upwards around the generator and leaves the housing at the top before mixing into the suction line after the evaporator exit.

In order to identify H_1 (see Figure 3), a parametric study was carried out. Based on operating conditions described in Table 1 and a target minimum liquid height of 10 mm, H_1 was found to be 156 mm. As displayed in Figure 10, the liquid height increases with a decreasing ambient temperature and increasing indoor temperature. The two curves shown on Figure 10 show this relationship for a cycle with two different combinations of expander isentropic efficiency, compressor suction superheat, and condenser outlet subcool. Several other parametric studies over ranges of these three variables resulted in the lowest liquid height for a given ambient and indoor temperature occurring at the lowest expander isentropic efficiency, the highest superheat, and the lowest condenser outlet subcool allowed by the ranges of values outlined in Table 1, with the highest liquid level occurring at the opposite extrema. Therefore, the two curves represent the two extreme cases showing the relationship of liquid height in the housing with respect to ambient and indoor temperature. The maximum liquid height that can be reached based on the described conditions is 64.4 mm. With a liquid height of 64.4 mm, the distance between the top of the liquid and the turbine bottom was found to be 91.4 mm. Using these dimensions, it was deemed that safe operation could be achieved for all defined operating conditions.

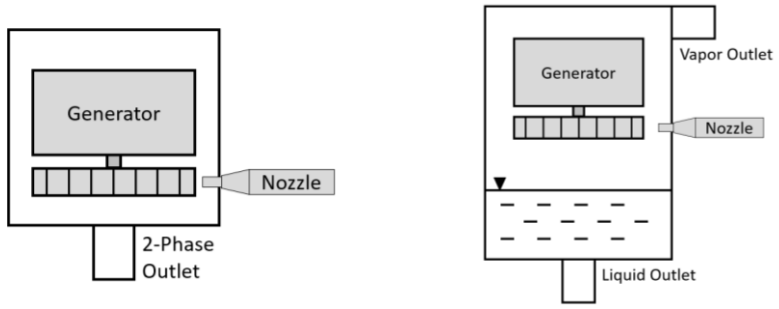

a) Initial expander housing b) Modified expander housing

Figure 9: Comparison of expander housing schematics

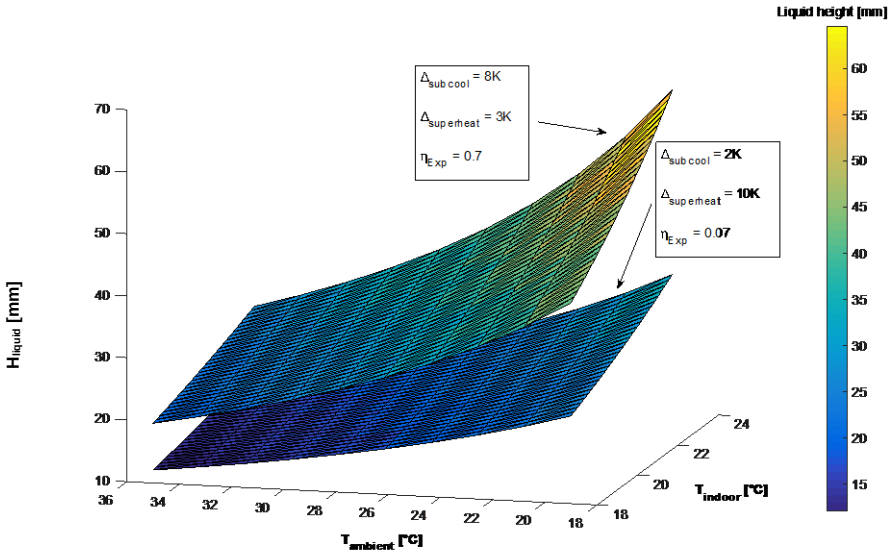

Figure 10: Liquid height in housing vs. $T_{ambient}$ and T_{indoor}

4.3 Expander Testing Results

The experimental results were obtained by operating the heat pump system in cooling mode with expander engaged and vapor bypass line partially open at test conditions A and B according to ANSI/AHRI Standard 210/240 (2008). The expander featured a C-D nozzle with a throat diameter of 2.79 mm. To ensure measurable levels of compressor suction superheat and condenser outlet subcool, the vapor bypass valve that bypasses the evaporator and injects saturated vapor into the suction line was opened as far as possible without sending two-phase refrigerant into the compressor suction. P-h diagrams for expander operation under test conditions A and B are shown in Figure 11.

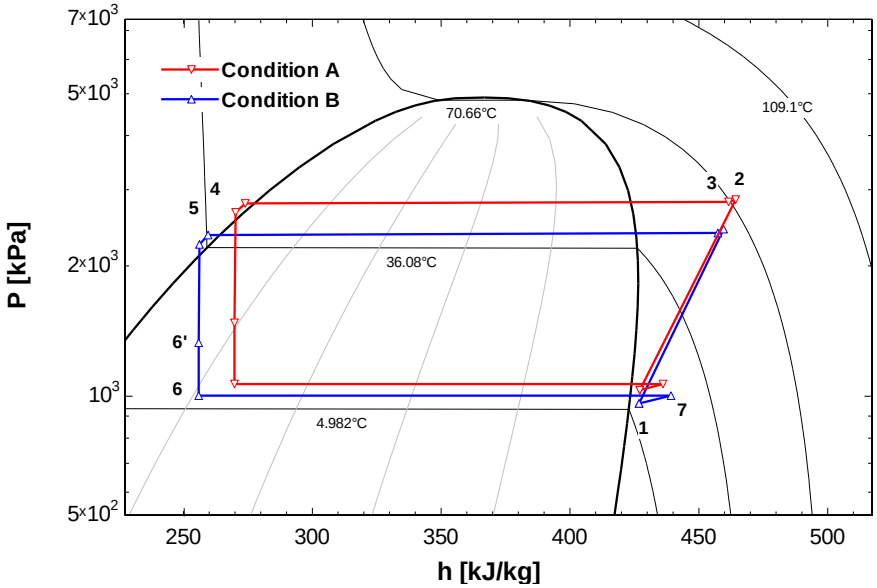

Figure 11: Expander heat pump cycle at operating conditions A and B in a P-h diagram

It should be noted that the phase separation is not displayed on these P-h diagrams, rather the expander outlet is simply set as State 6' and the evaporator distributor outlet and evaporator inlet is State 6. This is because the sight glasses installed at the saturated liquid and saturated vapor outlets of the expander showed significant bubbles, suggesting that the phase separation within the expander needs to be improved before saturated states can be assumed. Additionally, it is important to differentiate the expander outlet from the distributor outlet, as there is a significant pressure drop across the evaporator distributor, which is not available for expansion work recovery. Therefore, if the entire pressure drop from State 5 to State 6 was considered in the calculation of isentropic expansion work available for recovery, the resulting isentropic efficiency of the expander would be a significant underestimation of the actual performance of the device.

Due to the higher condensing temperature, test condition A has higher potential energy available for work recovery than test condition B. At condition A, with the vapor bypass valve partially open, the expander produced 45 W at 4983 rpm, resulting in an overall isentropic efficiency of 17%. While test condition B has a lower pressure differential than test condition A, the expander inlet density is lower than at test condition A. At test condition B, the expander produced 31 W at 4035 rpm with a partially opened vapor bypass valve, but achieved an isentropic efficiency of 18%. These results are in agreement with the findings of previous expander analyses performed by Czapla *et al.* (2016) that the expander performance is inversely related to inlet density, suggesting a higher sensitivity to increasing the velocity of the flow than increasing the inlet density.

The further the vapor bypass valve is opened the more power is output from the expander. However, this also decreases both the compressor suction superheat as well as the evaporation pressure. While experiments have shown significant power production from the expander with the vapor bypass valve open completely, the compressor suction superheat and condenser outlet subcool often disappeared, suggesting further development of nozzle and vapor bypass valve selection is necessary before results can be confidently presented.

5. CONCLUSIONS

This paper presented an explanation of both experimental and theoretical analyses conducted in an effort to redesign the housing of the Viper Expander for application in an R410A heat pump. These modifications resulted in a device that acts as both an expansion work recovery device and an open economizer. Flow visualization experiments led to modification of the nozzle position to increase the effectiveness of the turbine at harnessing kinetic energy from the flow. The inner diameter of the housing was increased to allow more space for liquid to separate from the turbine, and separate outlets at the top and bottom of the housing were implemented to facilitate further phase separation in the turbine. Both of these efforts were made with the intention of removing liquid from the turbine quickly in order to reduce frictional losses, and the modification with separate outlets for both phases creates another possible avenue for cycle control with an expansion work recovery device via vapor bypass flow rate modulation. Preliminary results show an expander isentropic efficiency of up to 18%. Future work includes iterating on nozzle diameter and type to balance maintaining compressor suction superheat and condenser outlet subcool while also increasing the amount of saturated vapor that can be removed from the expander housing to bypass the evaporator. Improving phase separation in the flash tank portion of the expander will also be a focus of the future work.

ACKNOWLEDGEMENTS

The authors would like to thank Regal Beloit Corporation financial and technical support for this project, as well as the faculty and staff of Ray W. Herrick Laboratories.

REFERENCES

ANSI/AHRI Standard 210/240 (2008) with Addendum 1.

Baek, J.S., Groll, E.A., Lawless, P.B. (2002). Development of a Piston-Cylinder Expansion Device for the Transcritical Carbon Dioxide Cycle. *Proc. Of the Int'l Compressor Eng. Conf. at Purdue,* Paper 584, West Lafayette, IN, 2002.

Czapla, N., Inamdar, H., Salts, N., Groll, E.A. (2016) Performance Testing of Unitary Split-System Heat Pump with an Energy Recovery Expansion Device. *Proc. Of the Int'l Compressor Eng. Conf. at Purdue,* Paper 1790, West Lafayette, IN.

He, T., Xia, C., Zhao, Y., Li, L., Shu, P. (2009). An Experimental Study on Energy Recovery by a Pelton-Type Expander in a Domestic Refrigeration System. *HVAC&R Research, 15:4, 785-799.*

Klein, S., "Engineering Equation Solver", F-Chart Software, v. 10.268, 2018.

Sakata, H., Nagatomo, S., Matsuzaka, T. (1984). Turbine for Use in Refrigeration Cycle. U.S. Patent No. 4,442,682.

Tondell, E. (2006). Impulse Expander for CO_2. *Proc. of 7th IIR Gustav Lorentzen Conference*, Trondheim, Norway, May 28-31, 2006.

Wang, M., Zhao, Y., Cao, F., Bu, Gaoxuan, B., Wang, Z. (2012). Simulation Study on a Novel Vane-Type Expander with Internal Two-Stage Expansion Process for R-410A Refrigeration System. *International Journal of Refrigeration, 35:4, 757-771.*

Wang, X., Hwang, T, Radermacher, R. (2009). Two-Stage Heat Pump System with Vapor-Injected Scroll Compressor Using R410A as a Refrigerant. *International Journal of Refrigeration, 32:6, 1442-1451.*

Zhang, Z., Tian, L. (2014). Exergy Analysis of a Subcritical Refrigeration Cycle with an Improved Impulse Turbo Expander. *Entropy, 16:8, 4392-4407.*

NOMENCLATURE

N	Number	(-)	**Acronyms**	
R	Radius	(m)	HVAC&R	Heating, Ventilation, Air Conditioning and Refrigeration
k_1	Disc Friction Coefficient	(-)	HFC	Hydrofluorocarbon
k_2	Rotor Shape Coefficient	(-)	TXV	Thermostatic Expansion Valve
H	Height	(m)	EXV	Electronic Expansion Valve
p	Pressure	(kPa)	AC	Alternating Current
h	Specific Enthalpy	(kJ/kg)	DC	Direct Current
T	Temperature	(°C)	COP	Coefficient of Performance
s	Specific Entropy	(kJ/kg-K)	EES	Engineering Equation Solver
$\dot{W}$	Power	(W)	C-D	Converging-Diverging
$\dot{m}$	Mass Flow Rate	(kg/s)		
D	Diameter	(m)	**Subscript**	
			comp	Compressor
Greek Symbols			out	Outlet
ρ	Density	(kg/m^3)	in	Inlet
ω	Rotational Velocity	(rpm)	s	Isentropic
η	Isentropic Efficiency	(-)	exp	Expander
			1,2,3…	State Points/Number on Schematic
			t	Turbine
			h	Housing
			exp,o	Overall Expander Isentropic Efficiency